Volume 770:25-43





Deep-sea nematode community changes over two decades at HAUSGARTEN observatory (Fram Strait, Arctic Ocean)

Jannik Schnier^{1,*}, Thomas Soltwedel¹, Katarzyna Grzelak², Barbara Górska², Jennifer Dannheim¹, Vadim Mokievsky³, Pedro Martínez Arbizu⁴, Christiane Hasemann¹

¹Alfred Wegener Institute Helmholtz-Centre for Polar and Marine Research, Am Handelshafen 12, 27570 Bremerhaven, Germany

²Institute of Oceanology, Polish Academy of Sciences, ul. Powstańców Warszawy 55, 81-712 Sopot, Poland ³P.P. Shirshov Institute of Oceanology, Russian Academy of Sciences, Nakhimovsky prosp. 36, Moscow 117997, Russia ⁴German Centre for Marine Biodiversity Research (DZMB), Senckenberg am Meer, Südstrand 40, 26382 Wilhelmshaven, Germany

ABSTRACT: Over the past 2 decades, deep-sea nematode communities in the Arctic Ocean have undergone significant changes in structure and diversity, likely linked to shifting organic matter input and environmental conditions. Free-living nematodes were collected in 2000, 2004, 2009, 2014 and 2019 at 3 stations along a bathymetric transect (1300, 2500, 4000 m) at the Long-Term Ecological Research (LTER) observatory HAUSGARTEN, a region of the Arctic Ocean undergoing rapid environmental change. Nematodes were identified to genus level and their biomass size distribution was calculated. Sedimentary food indicators, i.e. chloroplastic pigments (phytodetritus) and bacterial abundance/biomass, were analysed as explanatory variables. Food availability changed over time, with initial chlorophyll a decline at shallower depths, followed by increasing total pigment concentrations and bacterial biomass at greater depths, especially at 4000 m. Nematode abundances declined significantly across all depths, most notably by ~75% at 1300 m. Multivariate analyses revealed progressive and significant shifts in community composition, influenced primarily by depth and with clear separation between early (2000) and late (2019) samples. Alpha diversity (EG(50), J', H'(log2)) declined over time, remaining highest at 1300 m. Beta diversity based on genus exchange ratios showed high genus turnover (29-77%) and changes in dominance (12-55%), suggesting a combination of immigration and replacement of rare genera. Our findings indicate that long-term warming in surface waters and an accompanying shift in productivity are potentially reshaping deep-sea nematode communities, particularly at bathyal depths. This study highlights the value of sustained long-term time-series for understanding deep-sea benthic responses to climate change.

KEY WORDS: LTER HAUSGARTEN · Meiofauna · Benthos · Time series · Diversity · Biomass · Environmental change · Arctic Ocean

1. INTRODUCTION

Small-bodied meiofauna, defined as organisms captured by sieves with mesh sizes between 32 and 500 μm , can be found in almost every habitat on our planet in

high abundances and with great taxonomical and functional diversity (Schratzberger & Ingels 2018). Meiofauna contributes to a variety of marine benthic ecosystem processes in ways such as the following: the enhancement of sediment porosity, thereby increas-

ing vertical nutrient and oxygen fluxes; an increase in remineralisation rates; and by making the production of the microscopic realm accessible to higher trophic levels (Montagna 1995, Coull 1999, Schratzberger & Ingels 2018).

In deep-sea sediments (>300 m water depth), freeliving nematodes often dominate the metazoan meiofauna in terms of abundance, biomass and diversity (Wolff 1977, Vanhove et al. 1995, 2004, Shimanaga & Shirayama 2000, Baguley et al. 2008, Grzelak et al. 2017). Despite their dominance, nematode communities are not uniform, and their composition is strongly influenced by food availability (Danovaro et al. 2013). With the exception of chemosynthetic systems, the deep-sea benthos is dependent on organic matter that is produced in the euphotic zones of the oceans and exported to the sediments, often in seasonal pulses and resulting in a patchy distribution (Smith et al. 2008). While some deep-sea nematodes have a predatory lifestyle, the majority feed upon microbes and phytodetritus (Heip et al. 1985, Jensen 1988, Soetaert & Heip 1995, Ingels et al. 2011, Grzelak et al. 2017, Armenteros et al. 2022, Schnier et al. 2023), either directly on settling organic matter or indirectly by feeding on microorganisms associated with decomposing organic matter. Experimental studies have shown that nematodes prefer bacteria over phytodetritus (Gerlach 1978, Ingels et al. 2010) and that the presence of nematodes enhances remineralisation rates of detritus by keeping the bacteria in their exponential growth state which increases bacterial nitrogen fixation and methane oxidation in the sediments (Guden et al. 2024).

Despite their important role in benthic remineralisation processes, the distribution and ecological patterns of nematode communities across different deep-sea regions remain poorly understood. This is particularly true in the Arctic Ocean (Bluhm et al. 2011, Ramirez-Llodra et al. 2024), where the challenges of sampling deep-sea sediments are compounded by ice cover and remoteness. One of the better investigated regions of the Arctic Ocean is the highly productive marginal ice zone of the Fram Strait between Svalbard and Greenland. There, the Long-Term Ecological Research (LTER) observatory HAUS-GARTEN was established in 1999 to investigate natural and anthropogenically induced changes in the Arctic marine ecosystem (Soltwedel et al. 2005, 2016). The long-term analysis of the upper water column of HAUSGARTEN revealed that the surface water temperature has increased on average 0.06°C yr⁻¹ since 1997 (Beszczynska-Möller et al. 2012, R. McPherson et al. unpubl. data). This has led to significant changes

in the composition of the phytoplankton communities (Bauerfeind et al. 2009, Lalande et al. 2013, Nöthig et al. 2015, 2020), which has changed the organic matter supply to the sediments and thus directly affects the food availability for the meiobenthos. Soltwedel et al. (2020) investigated the abundance and diversity of major meiofauna taxa over a 15 yr time span along a bathymetric transect in HAUSGARTEN and found a decreasing trend in nematode abundances with time. Time-series study of nematodes (genus level identification) at HAUSGARTEN to date has encompassed 2 studies with time spans of 5 yr each (Hoste et al. 2007, Grzelak et al. 2017).

The aim of the present study was to build upon the previous investigations of nematode genera by extending the time series to cover a 20 yr period, analysed in 5 yr intervals. Specifically, we aimed to assess whether the declining trend in nematode abundance reported by Soltwedel et al. (2020) has persisted and to examine temporal changes in nematode diversity and biomass. Additionally, we evaluated long-term patterns in food availability for nematodes in the HAUSGARTEN area, its influence on benthic nematode communities, and whether these patterns varied with water depth.

With regard to the previous time-series investigations, we formulated the following research questions:

- (1) How have key sedimentary food-availability parameters (chloroplastic pigments indicating phytodetritus, bacterial abundance/biomass) changed over the 20 yr time series at HAUSGARTEN, and to what extent do these changes explain temporal and spatial variation in nematode community structure?
- (2) Have nematode communities at HAUSGARTEN exhibited significant temporal changes in abundance, biomass and diversity over the past 20 yr, potentially in response to variations in food availability?
- (3) Have nematode communities at HAUSGARTEN exhibited significant spatial changes in abundance, biomass and diversity with water depth?

2. MATERIALS AND METHODS

2.1. Study site, sampling and sample processing

The study site was the LTER observatory HAUS-GARTEN, located in the Fram Strait at about 78—80°N to 05°W—11°E between Greenland and the Svalbard archipelago (Soltwedel et al. 2005). Fram Strait is the only deep-water connection between the Arctic and Atlantic Ocean. Its bathymetry ranges

from shelves and slopes off Greenland and Svalbard to bathyal and abyssal depths in the Hovgaard Fracture Zone, the Molloy Fracture Zone, the Spitsbergen Fracture Zone and the Molloy Hole at 5600 m depth (Klenke & Schenke 2002).

Sampling was carried out with the German research icebreaker RV 'Polarstern' (Knust 2017) during 5 expeditions to HAUSGARTEN in the Arctic summers of 2000 (ARK-XVI/2; Krause & Schauer 2001), 2004 (ARK-XX/1; Budéus & Lemke 2007), 2009 (ARK-XXIV/2; Klages 2010), 2014 (PS85; Schewe 2015), and 2019 (PS121; Metfies 2020). For this study, we considered the HAUSGARTEN stations HG-I, HG-IV and HG-VII at water depths of approximately 1300, 2500 and 4000 m, respectively (Fig. 1). Sampling at HG-VII is challenging due to the comparably steep seafloor, resulting in unsuccessful sampling of that station in 2009 and 2014.

A multiple corer (MUC) was deployed once at each station to obtain virtually undisturbed sediment samples. Three pseudo-replicate subsamples of the top 5 cm of the sediments were taken from different (randomly selected) cores from individual MUC hauls for nematode identification and measurement of chloroplastic pigments. Sedimentary bacteria were sampled with 1 subsample per MUC haul. The subsamples for nematode identification and subsamples for biogenic parameter analysis could be taken from different cores of the same MUC haul. Subsamples for nematode identification were collected with 2.2 cm diameter cut-off syringes, whereas subsamples for the analysis of biogenic parameters indicating food availability for nematodes (see Section 2.1.1) were collected with 1.2 cm diameter cut-off syringes. Nematode subsamples were sliced in 1 cm layers and fixed in borax-buffered 4% formalin/filtered seawater solution (v/v). Sediment subsamples for the analysis of parameters indicating food availability to the nematodes (see Section 2.1.1) were also sectioned by centimetre and either processed directly on board or stored in 2% borax-buffered formalin/filtered seawater solution (v/v) for later analyses in the laboratory.

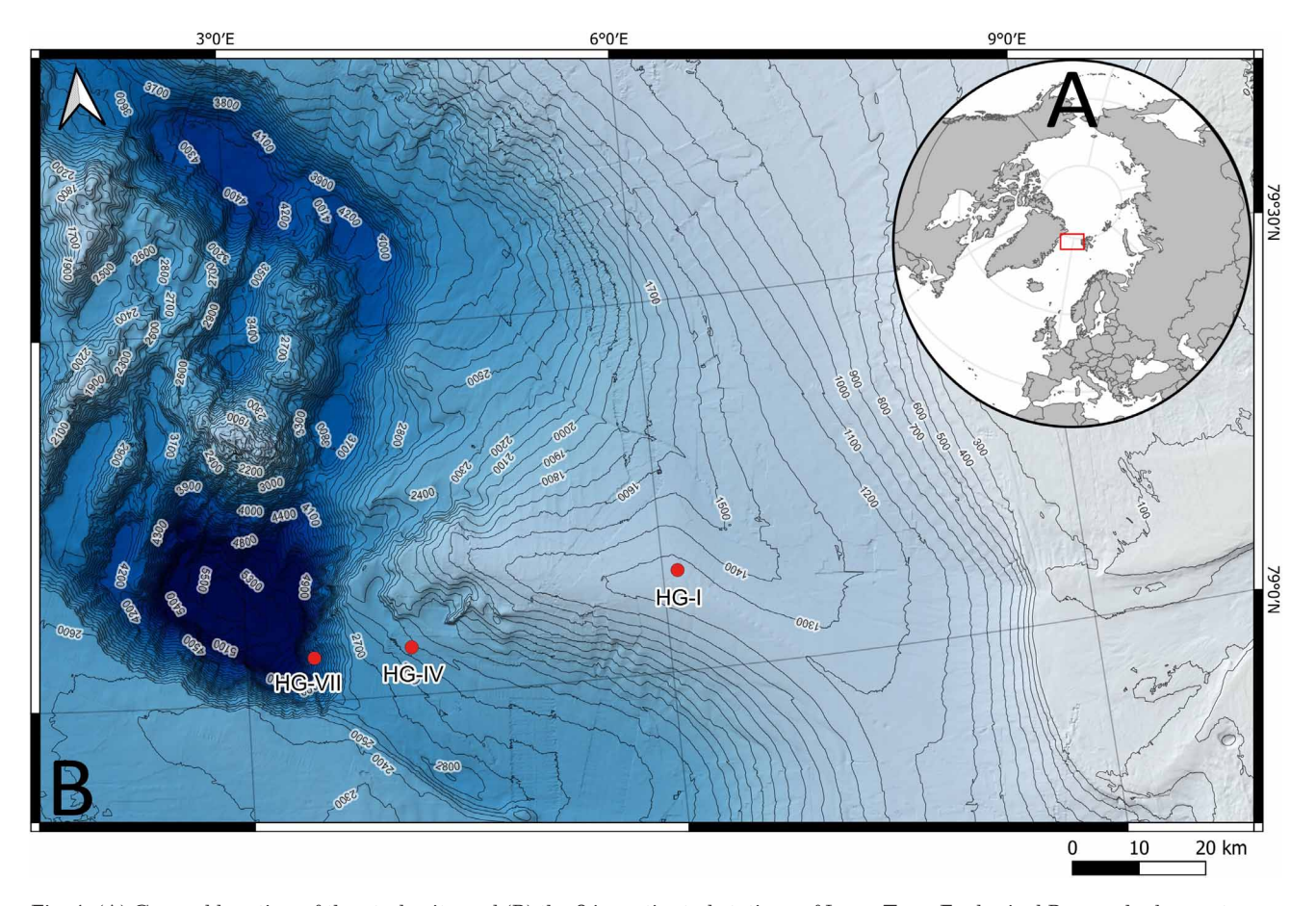


Fig. 1. (A) General location of the study site and (B) the 3 investigated stations of Long-Term Ecological Research observatory HAUSGARTEN: HG-I at ca. 1300 m depth, HG-IV at ca. 2500 m depth and HG-VII at ca. 4000 m depth (basemap: GEBCO Bathymetric Compilation Group 2023)

2.1.1. Parameters indicating food availability to sediment-inhabiting nematodes

For the present study, we investigated 2 proxies of potential food sources for nematodes. As the first proxy, we used the concentrations of sediment-bound pigments (chloroplastic pigment equivalents [CPEs], which comprise intact chlorophyll a [chl a] and its degradation products, i.e. phaeopigments [Phaeo], in μg ml⁻¹), indicating the availability of phytodetrital matter in the sediments. In the subsequent statistical analysis, the relative amount of chl a [%Chl] of the CPEs, as well as the total phaeopigment concentration were considered. As the second proxy, we used the density and biomass of sediment-inhabiting bacteria (total bacterial number, TBN [cells \times 10 8], and total bacterial biomass, TBB [µg C]). Unfortunately, bacterial data were not available for the year 2000 and only the uppermost sediment centimetre was available for bacterial analyses at all stations and years.

'Fresh' phytodetrital matter (indicated by intact chl *a*) and degraded phytodetrital matter (indicated by the bulk of phaeopigments) were estimated from pigment contents extracted from the sediments with 90% acetone. Concentrations of the different pigment types were then measured in a Turner fluorometer (Yentsch & Menzel 1963, Holm-Hansen et al. 1965).

TBN and TBB were determined from sediment samples fixed in 2% borax-buffered formol/filtered seawater solution (v/v). Cell counts and volume measurements were performed under an epifluorescence microscope after staining with acridine orange (Strugger 1948). TBB was estimated by calculating the cell volume of 50 randomly picked bacterial cells per sample as $\pi/4 \times W^2 \times (L-W/3)$, where L is bacterial length and W is bacterial width and applying the conversion factor of 3×10^{-13} g C μ m⁻³ to the average cell volume (Bratbak 1985, Børsheim et al. 1990).

The HAUSGARTEN time series data on food parameters for the years 2000—2015 are accessible on Mendeley Data (Hasemann & Soltwedel 2024); for 2016—2019, see Part 1 of Supplement 1 at www.int-res.com/articles/suppl/m770p025_supp1.xlsx.

2.1.2. Nematode preparation, taxonomic classification and biomass determination

The samples in this study were processed using the same methods in each year of the time series (see e.g. Hoste et al. 2007, Grzelak 2015, Grzelak et al. 2017, Schnier et al. 2023). Nematode samples were rinsed in fresh water through a 32 μ m sieve to remove the

excess formaldehyde. Extraction of nematodes (and other meiofauna taxa) from the sediments was achieved by density gradient centrifugation in a colloidal silica solution (LUDOX® TM-50, Sigma-Aldrich 420778; specific gravity of 1.18 g cm⁻³) for 15 min at 900 rpm (for method, see Heip et al. 1985). Each sample was centrifuged twice. After each centrifugation, the supernatant was rinsed with fresh water through a 32 µm sieve to remove the LUDOX®, and the meiofauna retained by the sieve were transferred to a Petri dish with freshwater and stained with Rose Bengal. The sorting was carried out under a stereomicroscope, and all nematodes were transferred to anhydrous glycerine. After glycerine infiltration, all nematodes were hand-picked and mounted on permanent slides for morphological genus identification and body size measurements for biomass estimations (see Pfannkuche & Thiel 1988).

Identification and body size measurements for biomass calculations were performed using a light microscope equipped with a digital camera. The keys of Platt & Warwick (1983, 1988), Warwick et al. (1998) and Schmidt-Rhaesa (2014) together with original descriptions were used to assign specimens to nematode genera. Nematode biomass was estimated from measuring individual body length (L) and body width (W). Total wet weight (wt) of nematodes was calculated using the formula of Andrássy (1956): $wt [\mu g] = L \times$ W^2 / 1600 000, where L is the nematode body length in μ m (excluding filiform tails) and W is the maximum body width in µm. Wet weight was converted to dry weight ($\mu g 10 \text{ cm}^{-2}$), assuming a dry to wet weight ratio of 0.25 (Wieser 1960). We log₂-transformed the nematode dry weight (rounded to the nearest decimal) to reveal the distribution of biomass across differently sized nematodes. Resulting log₂-size classes were plotted against the nematode dry weight (µq) in scatterplots (Schwinghamer 1981, 1983). Change in biomass distribution across size classes over time, along with the total size class range, indicate shifts in the relative abundance of smaller r-strategists in comparison to larger K-strategists within the community. Body size measurements are not available for HG-IV in 2000, all stations in 2004, and HG-VII in 2014.

Nematode data for the years 2000 and 2004 are based on published data sets from Hoste et al. (2007) and from Grzelak (2015) for 2009. For the latter study, Grzelak (2015) re-identified the original nematode specimens of Hoste et al. (2007); thus, we use the updated abundance data set of Grzelak (2015) in the present study. All abundance data from 2000—2009 were harmonized with the new count data from 2014 and 2019, which is accessible in 2 different data sets at PAN-

GAEA (Schnier et al. 2025a,b) and also contain body size measurements, biomass data and station metadata. Biomass data for the years 2000 and 2009 can be found in Part 2 of Supplement 1. Taxonomy and AphiaIDs are given in accordance with Schmidt-Rhaesa (2014) and the World Database of Nematodes (Nemys Eds. 2023). Synonyms in the older data were merged with accepted genus names in the newer data where appropriate.

2.2. Data analysis

Nematode abundances and sedimentary biogenic parameter data were standardized to an area of 10 cm⁻² prior to analyses. Abundances were visualized with scatterplots. Kruskal-Wallis tests (Kruskal & Wallis 1952) with post hoc tests (Dunn 1961) were performed to identify potentially significant differences in abundances between the investigated years for each station, respectively.

Multivariate statistics were performed using nonmetric multidimensional scaling (nMDS) on a Bray-Curtis similarity matrix of square-root transformed nematode abundance data to visualize the differences of nematode communities between years and stations (i.e. water depth). A permutational multivariate analysis of variance (PERMANOVA) was performed to test for significant differences (9999 permutations, alpha = 0.05) between years and stations (Anderson et al. 2008). To test whether group differences occur because of the location of their centroids, the dispersion around their centroids or both, a subsequent permutational analysis of multivariate dispersions (PERMDISP) was performed. One sample of HG-VII in 2019 was removed from the calculation of the nMDS plot and the PERMANOVA/PERMDISP, as it contained only 3 nematode specimens and thus heavily biased the results.

Nematode α -diversity was calculated as a rarefaction for the expected number of genera for 50 individuals (EG₍₅₀₎) (Sanders 1968, Hurlbert 1971), by using Shannon diversity ($H'_{(\log 2)}$) (Shannon 1948) and the evenness of genus distribution (J') (Pielou 1966) for each station and year.

Nematode β -diversity was described as temporal turnover by calculating the genus exchange ratio (GER) sensu Hillebrand et al. (2018) which refers to the proportion of genera that differ between 2 time points of a time series. The GER consists of 2 different ratios: the richness-based GER (GER_r) is calculated from the presence and absence of genera, analogous to the similarity index proposed by Jaccard (1912). The abundance-based GER (GER_a) is calculated from

the relative abundance of genera, based on Wishart's similarity ratio and Simpson index (Hillebrand et al. 2018). Hillebrand et al. (2018) provided the following formulas:

$$GER_{r} = \frac{G_{imm} + G_{ext}}{G_{tot}}$$
 (1)

where G_{imm} is the number of immigrating genera (new in later sample), G_{ext} is the number of extinct genera (lost from previous sample), G_{tot} is the total number of genera in both samples, and:

GER_a =
$$\frac{\sum_{i} (p_{i} - p'_{i})}{\sum p_{i}^{2} + \sum p'_{i}^{2} - \sum p_{i} p'_{i}}$$
 (2)

where the differences in relative genus abundance between the first time point p_i and the second time point p_i are considered. Both ratios have a range between 0 and 1, where $GER_r = 0$ means that all genera persisted and $GER_r = 1$ means all genera were exchanged. $GER_a = 0$ means that genus identity and dominance structure did not change, whereas $GER_a = 1$ means that a complete replacement of genera occurred. A direct comparison of the GER_r and GER_a represents a strong indicator for a change in diversity (Hillebrand et al. 2018).

Both ratios were calculated as the consecutive GER_r and GER_a , i.e. as the incremental change from year i to the following year (i+1), which in our study refers to an actual time frame of 5 yr (e.g. from year 2000 to 2004). In addition, the cumulative GER_r and GER_a were calculated for all combinations of sampling years, i.e. all possible time intervals (5, 10, 15 and 20 yr), to analyse the accumulation of biodiversity change over time, i.e. the long-term change in turn-over between any sampling year (i) and any consecutive sampling year (j) (see e.g. Rishworth et al. 2020). The cumulative GER thus is the mean turnover rate for the respective time interval.

For interpreting the β -diversity results, it should be noted that both GERs, and the GER, in particular, are sensitive to singleton genera. The failure to find the singleton genera in other samples, however, could be due to chance, since the size of the baseline population is unknown. For the calculation of the GER, only the change in presence and absence of genera between 2 timepoints is considered; therefore, the GER, potentially overestimates the true rate of exchange. The GERs we have calculated therefore represent the maximum achievable exchange ratios under the assumption that the singletons are truly only found in 1 sample due to rarity and not due to sampling bias.

A distance-based linear model (DistLM) (selection criterion: Adjusted R², selection procedure: BEST, 9999 permutations) was used to investigate the relationships between nematode abundance and biogenic parameters. Individual subsamples for nematode abundance and sediment parameters for each year were investigated (3 per 'year × site' combination). We decided to replace the missing bacteria data for the year 2000 with averages calculated from the annual bacteria data of the HAUSGARTEN timeseries for each station from 2002 to 2019, as the calculation of the DistLM was not possible with missing values and the alternative would be to exclude the year 2000 from the analysis altogether. Before the DistLM was calculated, the sedimentary biogenic data were normalized and tested for collinearity to reduce redundancy in the model (cut-off $r_s > 0.8$). Collinearities between most pairs of parameters were weak and ranged between $r_s = -0.26$ and 0.32. However, the pair TBN and TBB showed a strong collinearity of $r_s = 0.99$, indicating a potential redundancy for modelling (see Anderson et al. 2008). Therefore, we decided to exclude TBN from the DistLM. Results of the DistLM are presented in a distance-based redundancy analysis (dbRDA).

All analyses, except for the Kruskal-Wallis and Dunn tests as well as the β -diversity calculations, were performed using PRIMER 6 (version 6.1.15) with the PERMANOVA+ add-on (version 1.0.5; Clarke & Gorley 2006, Anderson et al. 2008). Plots of the nMDS and dbRDA were generated using PRIMER 6. Scatterplots, lollipop plots, the HAUSGARTEN map, the Kruskal-Wallis and Dunn tests and the β -diversity calculations were performed using R (version 4.4.3; R Core Team 2023) in the RStudio environment (version 2023.06.1; Posit Team 2023) and the packages 'tidyverse' (Wickham et al. 2019), 'ggpmisc' (Aphalo 2022), 'ggpubr' (Kassambara 2023a), 'rstatix' (Kassambara 2023b), 'cowplot' (Wilke 2020), 'showtext' (Qiu 2023), 'resample' (Hesterberg 2022) and 'hrbrthemes' (Rudis 2020). The HAUSGARTEN map was created with QGIS v.3.30.1 (QGIS Development Team 2009) and the embedded world map was created with the R-package 'ggOceanMaps' (Vihtakari 2023).

3. RESULTS

3.1. Parameters indicating food availability

The relative contribution of chl a (%Chl) to the total pigment content (as CPE) was similar at all 3 stations, except for the first 2 years, i.e. 2000 and 2004 (Fig. 2A).

In 2000, the highest %Chl was found at HG-I with a mean of $53 \pm (SD)$ 22% and decreased in the following years to 12 ± 1 % in 2019. At HG-IV in 2000 and 2004, the %Chl was 17 ± 1 and 17 ± 9 %, respectively, and decreased slightly from 16 ± 3 % in 2009 to 11 ± 3 % in 2014 and 13 ± 0.2 % in 2019. At HG-VII, %Chl was lowest in comparison to the other stations. In 2000, mean %Chl was 10 ± 1 % and increased slightly in 2004 to 13 ± 5 % and decreased to 9 ± 2 % in 2019.

The total phaeopigment concentration (Phaeo) in 2000, averaging 53.2 \pm 22.5 μ g ml⁻¹ at HG-I, 57.9 \pm $2.5 \ \mu g \ ml^{-1}$ at HG-IV and $57.9 \pm 0.7 \ \mu g \ ml^{-1}$ at HG-VII, were almost identical at the 3 stations (Fig. 2B). In 2004, mean Phaeo concentrations differed among stations, with a strong increase at HG-I to 126.8 \pm 18.1 μ g ml⁻¹, a slight increase to $66.0 \pm 7.4 \,\mu$ g ml⁻¹ at HG-IV and a decrease to $22.5 \pm 0.5 \,\mu \text{g ml}^{-1}$ at HG-VII. The trend of increasing Phaeo concentrations continued in 2009, with a further increase averaging $329.1 \pm 29.9 \,\mu \text{g ml}^{-1}$ at HG-I and $140.2 \pm 21.9 \,\mu \text{g ml}^{-1}$ at HG-IV. In 2014. Phaeo concentrations slightly decreased at HG-I to 239.3 \pm 22.1 μ g ml⁻¹ but were still higher in comparison to HG-IV with 145.9 ± 29.3 μg ml⁻¹. In 2019, mean Phaeo concentrations increased at all 3 stations to 329.6 \pm 61.5 μ g ml⁻¹ at HG-I, to $189.0 \pm 17.7 \,\mu g \, ml^{-1}$ at HG-I and to $190.1 \pm$ 79.0 μ g ml⁻¹ at HG-VII.

Bacterial density (TBN) and biomass (TBB) showed a similar pattern over the years (Fig. 2C,D). In 2004, a TBN of 17.2 \times 10 8 cells and a TBB of 62.5 μg C was found at HG-I, a TBN of 14.4 \times 10 8 cells and a TBB of 61.1 μg C at HG-IV and a TBN of 10.0 \times 10 8 cells and a TBB of 34.1 μg C at HG-VII. In 2009, TBN and TBB increased at HG-I and HG-IV to 70.6 \times 10 8 cells and 228.8 μg C and to 49.1 \times 10 8 cells and 146.7 μg C, respectively. Bacterial density and biomass decreased in 2014 to 34.4 \times 10 8 cells and 102.7 μg C at HG-I and 10.8 \times 10 8 cells and 30.9 μg C at HG-IV. In 2019, TBN and TBB strongly increased at all stations to 91.9 \times 10 8 cells and 280.3 μg C at HG-I, 116.3 \times 10 8 cells and 363.6 μg C at HG-IV and 261.6 \times 10 8 cells and 847.6 μg C at HG-VII.

3.2. Nematode abundance

Nematode abundances in the upper 5 cm of the sediments decreased with increasing water depth, i.e. across stations. The variation in nematode abundance at each station described station-specific patterns over time (Fig. 3). After an initial increase of 2482 ± 1201 ind. 10 cm^{-2} in 2000 to 3077 ± 171 ind. 10 cm^{-2} in 2004 at the shallowest HAUSGARTEN site (HG-I, 1300 m

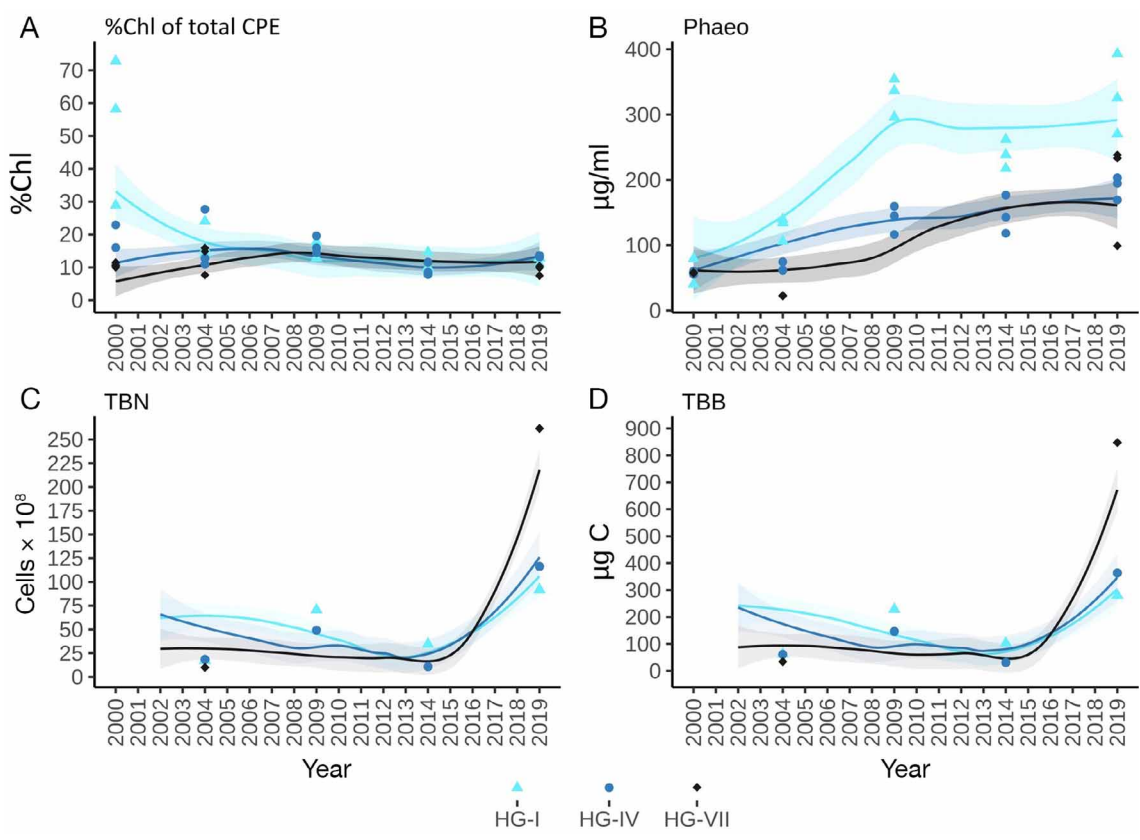


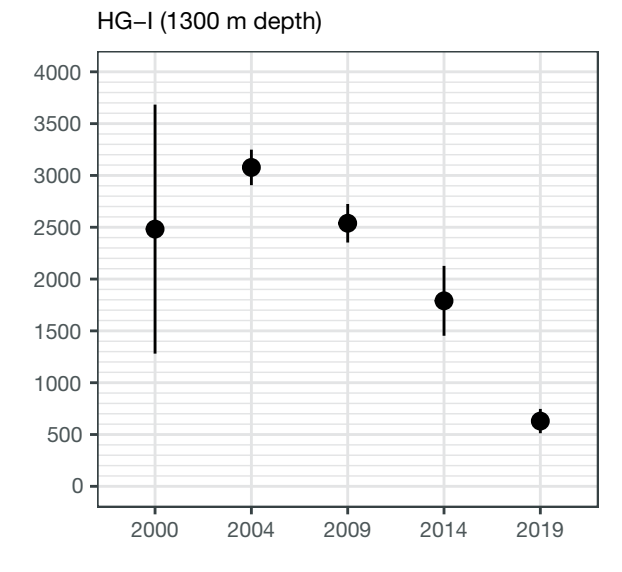
Fig. 2. (A) Percentage of chlorophyll a (%Chl) of the total pigment inventory (chloroplastic pigment equivalents, CPEs, (B) phaeopigment concentrations (Phaeo), (C) the total bacterial number (TBN) and (D) the total bacterial biomass (TBB) annually from 2000 to 2019 at Stns HG-I, HG-IV and HG-VII. Values are for the first sediment centimetre only (0-1 cm) and for an area of 10 cm^2 seafloor. Coloured, filled symbols show the years that were investigated in the present study with nematode data at the genus level. The trend lines are calculated as a LOESS-regression over the entire HAUSGARTEN time series with HG-I in light blue, HG-IV in dark blue and HG-VII in black and their respective standard deviations as faded background. For TBN and TBB, only 1 sample per station was taken and no bacterial samples were collected in 2000 and 2001. Additional information is available in Part 1 of Supplement 1

depth), mean nematode abundance gradually decreased over the years to 630 ± 117 ind. 10 cm^{-2} in 2019. This is a decrease in nematode abundance of 75% from 2000 to 2019. In comparison to 2019, nematode densities at HG-I were significantly higher in 2000 (p = 0.02), 2004 (p < 0.001) and 2009 (p = 0.003) (Table S1 in Supplement 2 at www.int-res.com/ articles/suppl/m770p025_supp2.pdf). At intermediate depths (HG-IV, 2500 m depth), the mean nematode abundance described a unimodal pattern, with a peak abundance of 1069 ± 131 ind. 10 cm^{-2} in 2009. Lowest abundances at HG-IV were found in 2019, with a mean of 261 ± 83 ind. 10 cm^{-2} . Between 2000 and 2019, the abundance decreased by 53%, while the strongest decrease was between 2009 and 2019 with 73%. The decrease in abundances between 2004 and 2019 (p = 0.014), as well as between 2009 and 2019 (p < 0.001) were significant. At HG-VII (4000 m depth), abundances decreased from 527 ± 336 ind. 10 cm^{-2} in 2000 to 121 \pm 13 ind. 10 cm $^{-2}$ in 2004 and 187 \pm 198 ind. 10 cm $^{-2}$ in 2019. This is a significant (p = 0.031) decrease by 66% between 2000 and 2019.

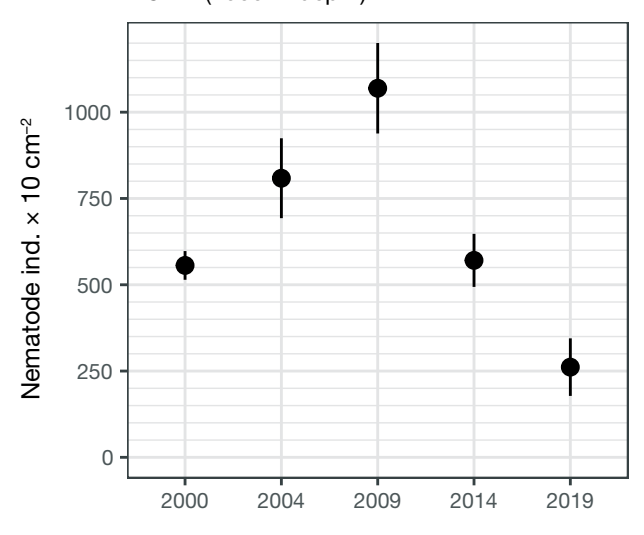
Nematode abundances per sediment layer generally decreased with increasing sediment depth for all years and stations (individual lollipops in Fig. S1 in Supplement 2). As an exception, abundances at HG-I in 2009 and 2014 were the highest in the 2-3 and 1-2 cm layers, respectively. The nematode abundance in the lowest sediment layer contributed 5% to the total abundance across all layers.

In 2014 and 2019, nematode life-stage information was available. The ratio of juveniles to adults was higher at both stations (HG-I and HG-IV) in 2014 in comparison to 2019 (Fig. S2 in Supplement 2).

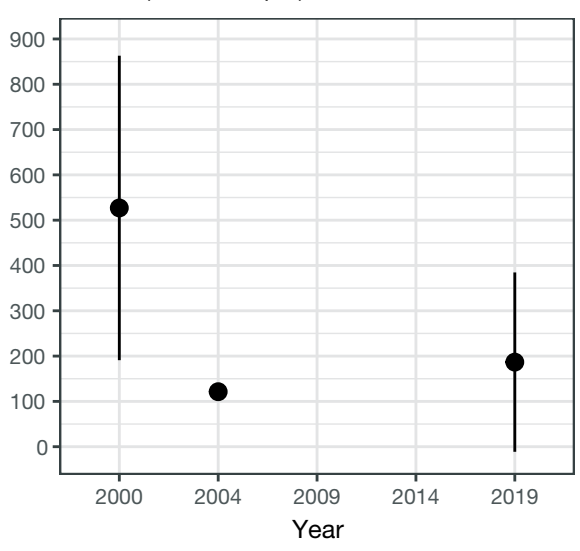
A multivariate analysis of the nematode abundance data revealed significant changes in the community composition over time and water depth (Fig. 4). Global PERMANOVA results showed that







HG-VII (4000 m depth)



water depth had a larger effect on nematode communities than time, but both factors were significant (Table 1). The pairwise test showed that all combinations of years (except 2000 × 2004) and all combinations of stations expressed a significantly different nematode community structure. The greatest differences were observed between 2000 × 2019, 2009 × 2014 and 2009 \times 2019, and between HG-I \times HG-IV and HG-I × HG-VII (Table 1). The PERMDISP revealed a significant difference in dispersion from the centroid of the years and the stations, respectively (Table 2). Pairwise comparisons showed significantly different variability in nematode community structure between the years 2000 × 2004, 2004×2014 , and 2014×2019 . For the stations, all pairwise combinations with HG-VII resulted in significantly different variability.

3.3. Nematode biomass

Total nematode biomass generally decreased with water depth. At HG-I, nematode biomass was distributed in size classes ranging from -10 to 4 over all investigated years (exception: 2004, since no biomass data) (Fig. 5A; Fig. S3A in Supplement 2). Biomass in the largest size classes 3 and 4 was exclusively found at HG-I and did not occur at the other 2 stations. Over time, the range of the nematodebiomass size-class spectra at HG-I varied slightly (2000: -10 to 3; 2009: -8 to 3; 2014: -10 to 3; 2019: -8 to 4) with the absence of biomass size-classes smaller than -8 in 2019. Highest nematode biomass was found in increasing size classes over time: 2000: $8.8 \pm 7.9 \,\mu g$ in size-class 1; 2009: $19.3 \pm 2.7 \,\mu g$ in size class 2; 2014: $8.6 \pm 0.0 \,\mu g$ in size class 3; 2019: $11.5 \pm$ 0.0 µg in size class 4. However, the biomass in size classes 3 and 2 in 2014 were attributed to single specimens of the genera Paramesacanthion and Sabatieria, respectively. In 2019, the biomass in size class 4 was attributed to a single specimen of the genus Anticoma. When these single occurrences were excluded, biomass in 2014 was highest in size class 1 and in 2019 in size class 2.

At HG-IV, nematode biomass was distributed in a size-class range from -9 to 1 in 2009, -10 to 1 in 2014 and -8 to 1 in 2019, indicating that no biomass

Fig. 3. Nematode abundance (ind. 10 cm⁻²) as the mean of 3 replicate samples plotted for each station and year. Error bars show SD. Note that the standard deviation for HG-VII in 2004 was 13 and thus the error bar is covered by the point

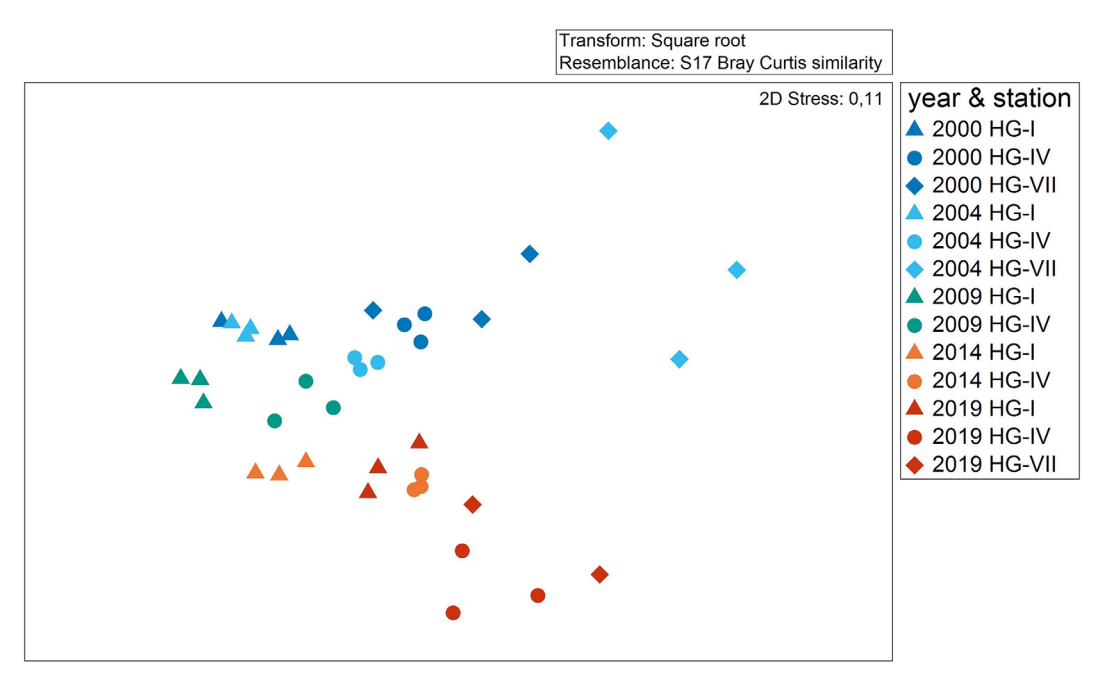


Fig. 4. Similarities (Bray-Curtis) among years and stations based on square-root transformed nematode abundance data plotted in a non-metric multidimensional scale (nMDS) ordination. Colours represent the different sampling years, symbols represent the 3 stations

 $\label{eq:permix} Table \ 1. \ Results \ of \ PERMANOVA \ on \ nematode \ abundance \ data \ for \ global \ and \ pairwise \ tests \ between \ years \ and \ stations. \ p_{\text{(perm)}}: \ p-value \ for \ permutation; \ p_{\text{(MC)}}: \ Monte-Carlo-corrected \ p-value$

Source	df	SS	MS	Pseudo-F	$p_{\left(perm\right) }$	Unique perms	$p_{(MC)} \\$
Year	4	21251	5312.7	7.1326	< 0.001	9877	< 0.001
Station	2	15095	7547.4	10.1330	< 0.001	9907	< 0.001
Year × Station ^a	6	12717	2119.5	2.8455	< 0.001	9828	< 0.001
Residuals	25	18621	744.85				
Total	37	70578					
^a Term has one or m	nore empty ce	ells					
PERMANOVA pai	rwise tests						
Groups	t	$p_{\left(perm\right) }$	Unique perms	$p_{(MC)}$			
2000, 2004	1.453	0.006	9927	0.055			
2000, 2009	2.213	< 0.001	9918	0.002			
2000, 2014	2.926	< 0.0001	9940	< 0.001			
2000, 2019	3.329	< 0.0001	9936	< 0.001			
2004, 2009	1.804	0.003	9932	0.013			
2004, 2014	2.706	< 0.001	9935	0.001			
2004, 2019	3.051	< 0.001	9943	< 0.0001			
2009, 2014	3.100	0.003	8934	0.001			
2009, 2019	2.977	0.001	9923	< 0.001			
2014, 2019	2.308	0.003	9908	0.003			
HG-I, HG-IV	3.771	< 0.0001	9913	< 0.0001			
HG-I, HG-VII	3.401	< 0.0001	9932	< 0.0001			
HG-IV, HG-VII	2.093	< 0.0001	9925	0.001			

was found in the smallest size classes in 2019 (Fig. 5B; Fig. S3B). Biomass data for 2000 and 2004 were unavailable at this station. The highest biomass was

observed in the 2 largest size classes each year: 2009: $4.6 \pm 2.8 \ \mu g$ in size class 1; 2014: $1.8 \pm 0.5 \ \mu g$ in size class 1; 2019: $5.4 \pm 4.4 \ \mu g$ in size class 0.

Table 2. PERMDISP test results of the nematode abundance data. The deviations from the centroids of the year and station groups were tested. $p_{(perm)}$: p-value for permutation

	df1	df2	F	$p_{(\text{perm})}$
Deviations from centroid (year):	4	33	4.585	0.028
Deviations from centroid (station):	: 2	35	8.622	0.004
Pairwise comparisons				
Groups	t	$p_{\left(perm\right) }$		
(2000, 2004)	1.634	0.198		
(2000, 2009)	1.248	0.288		
(2000, 2014)	2.768	0.017		
(2000, 2019)	0.199	0.860		
(2004, 2009)	2.167	0.172		
(2004, 2014)	3.023	0.050		
(2004, 2019)	1.791	0.197		
(2009, 2014)	1.929	0.080		
(2009, 2019)	1.527	0.206		
(2014, 2019)	3.948	0.004		
(HG-I, HG-IV)	17.131	0.153		
(HG-I, HG-VII)	42.648	0.001		
(HG-IV, HG-VII)	26.306	0.033		
Means and standard errors				
Group	Size	Average	SE	
2000	9	34.378	2.153	
2004	9	41.817	4.011	
2009	6	30.623	1.733	
2014	6	26.459	1.286	
2019	8	33.863	1.303	
HG-I	15	32.485	15.617	
HG-IV	15	36.488	17.382	
HG-VII	8	44.271	24.076	

At HG-VII, nematode biomass data were only available for 2000 and 2019. Biomass was distributed from size classes -11 to 2 in 2000 and -8 to 2 in 2019 (Fig. 5C). The highest biomass was observed in 2000 with 1.1 \pm 1.9 μg in size classes 1 and 2. In 2019, the highest biomass was noted in size class 2 with 10.7 \pm 0.0 μg , which was attributed to only 3 large individuals of the genus Parasphaerolaimus. When these were excluded, biomass in 2019 was highest in size classes -2 and 0 with 2.0 \pm 0.7 and 2.0 \pm 1.2 μg , respectively.

3.4. Nematode diversity

3.4.1. α -diversity

A total of 189 genera were identified across all years and stations. The relative abundance of the 10 most abundant genera (38 genera in total) per year and sta-

tion ranged between 58% in 2009 at HG-I and 82% in 2019 at HG-VII (Table S2 in Supplement 2). The range in relative abundance of the single most abundant genus per year and station ranged between 10 and 27%. The only 2 genera that were among the 10 most dominant genera at all stations and years were Acantholaimus and Tricoma; these genera always exceeded 5% of the total relative abundance. At HG-I, Acantholaimus, Aegialoalaimus, Desmoscolex and Tricoma were the only 4 genera which were among the 10 most dominant genera in all 5 years. At HG-IV and HG-VII, Acantholaimus, Halalaimus and Tricoma were the only genera that were among the dominant genera

The expected number of genera for 50 individuals (EG $_{(50)}$) over all years was highest at HG-I and lowest at HG-VII (Table 3). At HG-I, EG $_{(50)}$ increased from 21 ± 1 in 2000 and 22 ± 1 in 2004 to 23 ± 1 in 2014, and decreased to 18 ± 2 in 2019. At HG-IV, EG $_{(50)}$ was almost identical in all years with a range of 21 ± 1 in 2009 to 19 ± 4 in 2019. At HG-VII, EG $_{(50)}$ decreased across the years from 17 ± 2 in 2000 to 10 ± 3 in 2004 and 11 ± 7 in 2019.

Evenness (J') at HG-I was highest in 2000 and 2009, with 0.84 \pm 0.02 and

 0.86 ± 0.02 , respectively, and lowest in 2019 with 0.77 ± 0.03 (Table 3), whereas at HG-IV, evenness was highest in 2000 with 0.90 ± 0.05 and lowest in 2014 with 0.83 ± 0.01 . At HG-VII, evenness was highest in 2004 with 0.91 ± 0.02 and lowest in 2000 with 0.87 ± 0.08 .

Shannon diversity ($H'_{(\log 2)}$) at HG-I increased from 4.56 ± 0.10 in 2000 to 4.78 ± 0.06 in 2014, and then decreased to 4.05 ± 0.28 in 2019 (Table 3). At HG-IV, $H'_{(\log 2)}$ also increased initially from 4.39 ± 0.24 in 2000 to 4.46 ± 0.08 in 2009, before it decreased in 2014 and 2019 to 4.34 ± 0.04 and 4.16 ± 0.50 , respectively. At HG-VII, $H'_{(\log 2)}$ decreased over the years from 3.97 ± 0.34 in 2000 to 2.96 ± 1.22 in 2019.

3.4.2. β -diversity

Consecutive GERs. Throughout the study period, the consecutive GER_r showed clear patterns across all 3 stations, with generally increasing turnover over

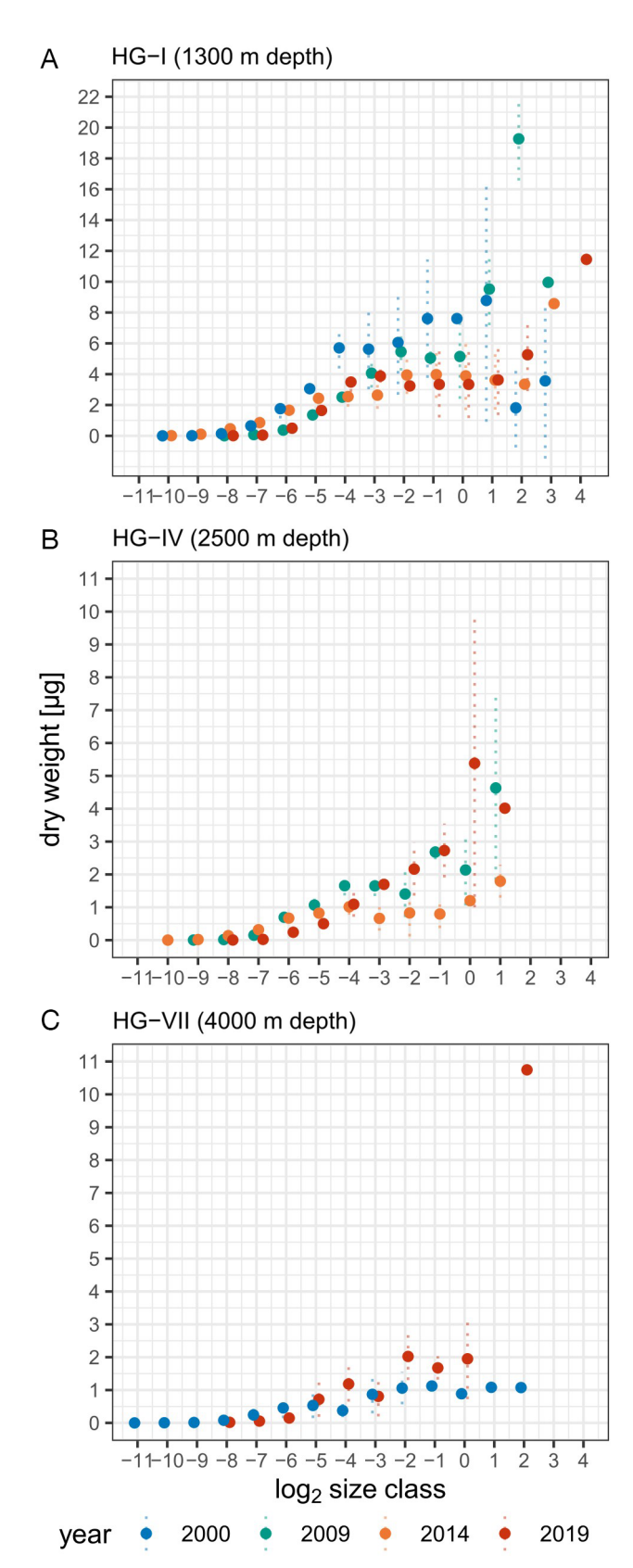


Fig. 5. Nematode biomass in μg per \log_2 -size class as a mean of the 3 samples per station and year. Dotted bars show standard deviation. Colours represent the different sampling years

time, especially at greater depths (Table 4). At HG-I (1300 m depth), genus replacement was initially relatively low, with about one-third of genera exchanged between 2000 and 2004. The exchange ratio increased to nearly 70% between 2009 and 2014, before slightly decreasing to around 60% in the final period from 2014 to 2019. A similar trend was observed at HG-IV (2500 m depth), where exchange rose from around 40% between 2000 and 2004 to about two-thirds between 2009 and 2014, followed by a moderate decline between 2014 and 2019. At the deepest station, HG-VII (4000 m depth), GER_r was consistently high. Around two-thirds of the genera were replaced between 2000 and 2004, and over three-quarters between 2004 and 2019, indicating the highest turnover among all sites and years.

Changes in consecutive genus dominance structure, as indicated by the abundance-based GER ar were generally smaller and more stable than the richness-based GER_r, but still showed notable patterns across stations (Table 4). At HG-I, changes in dominance were relatively minor early on, affecting less than 20% of the community between 2000 and 2004, and between 2004 and 2009, but gradually increased to around 30% between 2014 and 2019. At HG-IV, the strongest shifts in dominance structure occurred between 2000 and 2004 as well as between 2009 and 2014, while changes were minimal in the intervening and final periods. In contrast, HG-VII showed the most pronounced changes in GER_a overall, with about 40% of the community's dominance structure changing from 2000 to 2004, and over half changing between 2004 and 2019.

Cumulative mean GERs. The richness-based, cumulative mean GER_r indicated that on average up to 52–74% of genera were exchanged at each station between each time interval (Table 5). At HG-I, the mean GER_r was moderate to high, starting at 52% in the shortest (5 yr) interval and increasing to 70% in the 15 yr interval. Similarly, at HG-IV, the mean GER_r increased from 52% over 5 yr to 73% over 20 yr. In contrast, HG-VII consistently showed the highest mean turnover ratios, with 71% replaced in the shortest interval and reaching 74% over the longest interval.

The abundance-based, cumulative mean GER $_{\rm a}$ was overall lower than the mean GER $_{\rm r}$ and indicated a moderate to high change in genus identity and dominance structure of up to 22–66% over all time intervals and stations (Table 5). At HG-I, mean changes in dominance remained relatively stable at around 25% for the first 3 intervals, increasing more noticeably to a mean exchange of 43% over the 20 yr span. A similar trend was seen at HG-IV, though the mean exchange

Year	Station	G	N	$EG_{(50)}$	J'	$H'_{(\log 2)}$
2000	HG-I	44 ± 7	2199 ± 1069	21 ± 1	0.84 ± 0.02	4.56 ± 0.10
2004	HG-I	53 ± 7	2683 ± 160	22 ± 2	0.80 ± 0.03	4.60 ± 0.20
2009	HG-I	45 ± 3	2441 ± 186	23 ± 1	0.86 ± 0.02	4.72 ± 0.13
2014	HG-I	68 ± 3	1736 ± 320	22 ± 1	0.79 ± 0.02	4.78 ± 0.06
2019	HG-I	39 ± 6	624 ± 112	18 ± 2	0.77 ± 0.03	4.05 ± 0.28
2000	HG-IV	30 ± 2	455 ± 23	20 ± 2	0.90 ± 0.05	4.39 ± 0.24
2004	HG-IV	35 ± 2	710 ± 78	20 ± 1	0.86 ± 0.02	4.42 ± 0.07
2009	HG-IV	36 ± 3	999 ± 124	21 ± 1	0.87 ± 0.02	4.46 ± 0.08
2014	HG-IV	38 ± 2	553 ± 65	20 ± 1	0.83 ± 0.01	4.34 ± 0.04
2019	HG-IV	28 ± 10	260 ± 82	19 ± 4	0.88 ± 0.01	4.16 ± 0.50
2000	HG-VII	24 ± 3	440 ± 293	17 ± 2	0.87 ± 0.08	3.97 ± 0.34
2004	HG-VII	10 ± 3	87 ± 11	10 ± 3	0.91 ± 0.02	3.04 ± 0.44
2019	HG-VII	15 ± 13	186 ± 196	11 ± 7	0.89 ± 0.10	2.96 ± 1.22

Table 3. Nematode diversity indices calculated for the respective years and stations. G: mean number of genera; N: mean abundance; $EG_{(50)}$: expected number of genera for 50 individuals, J': Pilou's evenness; $H'_{(log2)}$: Shannon diversity. Data are mean \pm SD

Table 4. Consecutive (stepwise) nematode genus exchange ratios (GERs) for presence—absence-based turnover (GER $_{\rm a}$) and abundance-based turnover (GER $_{\rm a}$) across years and stations. Ratios in 2000 are set to NA (not applicable), since it was the start year and hence no exchange rate to a previous sample can be calculated

Year	Station	GER _r	GER _a
2000	HG-I	NA	NA
2004	HG-I	0.29	0.18
2009	HG-I	0.51	0.13
2014	HG-I	0.70	0.25
2019	HG-I	0.59	0.30
2000	HG-IV	NA	NA
2004	HG-IV	0.41	0.27
2009	HG-IV	0.52	0.13
2014	HG-IV	0.65	0.34
2019	HG-IV	0.55	0.12
2000	HG-VII	NA	NA
2004	HG-VII	0.65	0.41
2019	HG-VII	0.77	0.55

 $\label{eq:table 5. Mean \pm SD nematode genus exchange ratios (GERs) for presence-absence-based turnover (GER_r) and abundance-based turnover (GER_a) per time interval and station. NA: not applicable$

Interval	Station	GER_r	GER _a
1 (5 yr) 2 (10 yr) 3 (15 yr) 4 (20 yr) 1 (5 yr) 2 (10 yr) 3 (15 yr) 4 (20 yr) 1 (5 yr) 4 (20 yr)	HG-I HG-I HG-I HG-IV HG-IV HG-IV HG-VII HG-VII	0.52 ± 0.17 0.64 ± 0.14 0.70 ± 0.01 $0.67 \pm NA$ 0.53 ± 0.13 0.64 ± 0.10 0.70 ± 0.01 $0.73 \pm NA$ 0.71 ± 0.08 $0.74 \pm NA$	0.22 ± 0.07 0.25 ± 0.09 0.26 ± 0.14 $0.43 \pm NA$ 0.22 ± 0.08 0.29 ± 0.08 0.35 ± 0.17 $0.50 \pm NA$ 0.48 ± 0.10 $0.66 \pm NA$

ratios in the later intervals were slightly higher, suggesting shifts in up to half of the community's dominance structure. The most pronounced changes with highest mean GER $_{\rm a}$ occurred at HG-VII, where up to 50% of the dominance structure changed in the 5 yr interval and up to 66% over the full 20 yr interval.

3.5. Association between nematode communities and food availability in space and time

Mean bacterial density (TBN) values for 2000, calculated over all years for inclusion in the model, were 52.7×10^8 cells for HG-I, 47.6×10^8 cells for HG-IV and 50.2×10^8 cells for HG-VII. The calculated mean bacterial biomass (TBB) values for 2000 were 163.6 μ g C at HG-I, 145.6 μ g C at HG-IV and 152.0 μ g C at HG-VII.

The dbRDA explained 83.0% of the fitted DistLM variation and 15.3% of the total variation in the composition of the nematode communities of the uppermost centimetre of the sediments with the measured biogenic parameters (Fig. 6, Table 6). All biogenic parameters were significant predictor variables in the marginal tests. The DistLM revealed a different influence of the biogenic parameters on the nematode community structure over the years as well as over the depth gradient from HG-I to HG-VII. In 2000 and 2004, the variation in nematode communities at HG-I was best described by variation in %Chl, whereas in 2009, 2014 and 2019, combinations of %Chl and Phaeo were the best predictors. At HG-IV and HG-VII, the influence of the variation in %Chl and Phaeo on the variations in the nematode communities was smaller compared to HG-I for all years. In 2019, nematode

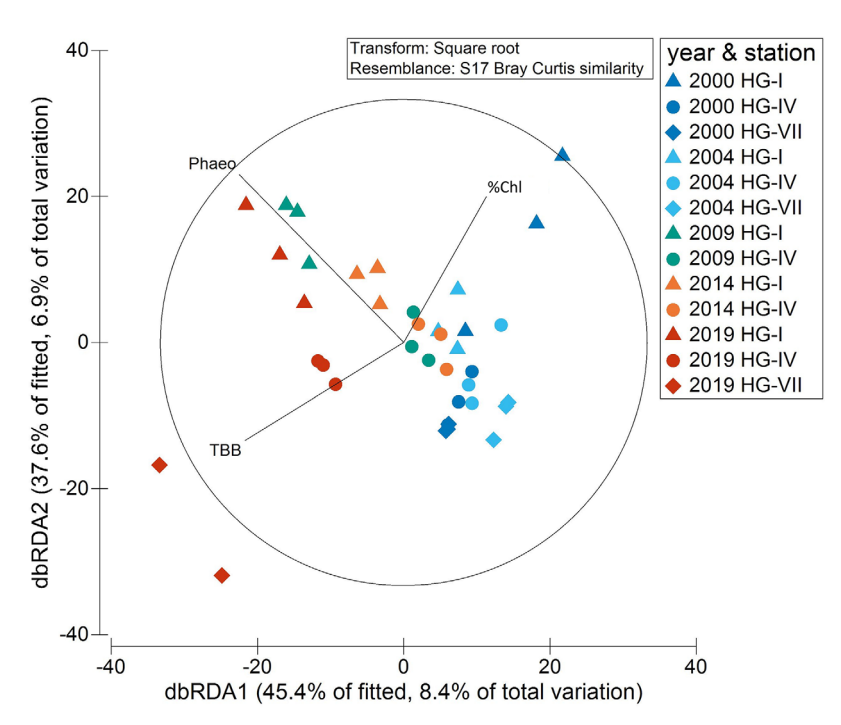


Fig. 6. Visualization of the results of a distance-based linear model (DistLM) with a distance-based redundancy ordination (dbRDA). The DistLM explains the variation in nematode communities with the variation in the different biogenic parameters of the first sediment centimetre (0–1 cm). Black lines and letters are the 3 different biogenic descriptor variables: %Chl: percentage of chlorophyll *a* of chloroplast pigment equivalents; Phaeo: phaeopigment concentration; TBB: total bacterial biomass. The black circle represents maximum possible vector length (unit circle). Colours represent the different sampling years, symbols represent the 3 stations

community structure at HG-IV and HG-VII was more affected by the variation in TBB compared to the other years.

4. DISCUSSION

4.1. Variations in food supply to deep-sea nematode communities at HAUSGARTEN

Previous studies have shown that food availability has a considerable significant effect on nematode diversity in deep-sea sediments (Zeppilli et al. 2015 and references therein). The data suggest that the drastic shift in the nematode communities observed over time in the present study may be at least partly due to a change in food quantity and potentially also quality. Deep-sea benthos is directly dependent on processes in the upper water column and can be affected by the input of organic matter (i.e. potential food) on time scales of days to weeks (Graf 1989). The sampling periods in this study varied between early June and mid-September, i.e. between different

times relative to possible phytoplankton blooms and phytodetritus input. Clearly, this has an effect on the consecutive degradation of organic matter and the possible subsequent benthic bacterial abundances, which rapidly react to an organic matter input and peak at HAUSGARTEN about 100 d after a phytoplankton bloom (Ramondenc et al. 2024). Nevertheless, the sedimentary phytopiqment concentrations during the sampling periods have been relatively constant since 2009 (Fig. 2). Thus, the significant changes in the nematode community in 2019 compared to previous years could be caused by changes in the quality of food — bacteria and organic matter available to the benthos.

Previous studies have found that the HAUSGARTEN euphotic zone underwent major variations in the plankton composition over the last 20 yr with a shift from a diatom-dominated community towards a flagellate- and coccolithophore-dominated community (Bauerfeind et al. 2009, Lalande et al. 2013, Nöthig et al. 2015, 2020). This shift in the phytoplankton community is associated with an overall continu-

ous increase in water temperatures of the water masses flowing from the Atlantic to the Arctic by 0.06°C yr⁻¹ between 1997 and 2010 (Beszczynska-Möller et al. 2012, R. McPherson et al. unpubl. data) and a series of marine heatwaves in the North Atlantic since 2003 (K.-M. Werner et al. unpubl. data). An ex situ experimental approach confirmed that the temperature fluctuations before, during and after a heatwave could strongly influence the Arctic phytoplankton community in terms of diversity and biomass production, with carry-over effects in community composition from one temperature phase to another (Wolf et al. 2024). Fadeev et al. (2021) found a 2-fold lower carbon export from the surface to the deep sea in flagellate-dominated communities of seasonal icefree areas at HAUSGARTEN (HG-I, HG-IV, HG-VII) compared to diatom-dominated communities in icecovered areas. These flagellates are mostly remineralised in the upper water column, but evidence suggests that agglomerations of the dinoflagellate Phaeocystis can reach deep sediments on short time scales by ballasting with ice-derived gypsum (Riebesell et al. 1995, Wollenburg et al. 2018, Swoboda et al.

Table 6. Results of the marginal tests and the BEST solutions of the distance-based linear model (DistLM) used to investigate the relationship between environmental variables and nematode communities. Prop.: explained proportion; TBB: total bacterial biomass; RSS: residual sum of squares; Vars: variables induced in the model

Marginal tests Variable	SS(trace)	Pseudo-F	p	Prop.
%Chl	3735.4	19.847	0.040	5.22×10^{-2}
Phaeo	5442.6	29.665	0.001	7.61×10^{-2}
TBB	4728.2	25.495	0.008	6.61×10^{-2}
BEST solutions				
BEST result for	each number of	variables		
Adj R ²	\mathbb{R}^2	RSS	No.Vars	Selections
5.047×10^{-2}	7.613×10^{-2}	66049	1	%Chl
8.327×10^{-2}	13.28×10^{-2}	61996	2	Phaeo; TBB
11.23×10^{-2}	18.43×10^{-2}	58320	3	%Chl; Phaeo; TBB
Overall BEST se	olutions			
Adj R ²	\mathbb{R}^2	RSS	No.Vars	Selections
0.11227	0.18425	58320	3	%Chl; Phaeo; TBB
0.083268	0.13282	61996	2	Phaeo; TBB
0.078789	0.12858	62299	2	%Chl; Phaeo
0.063146	0.11379	63357	2	%Chl; TBB
0.050466	0.076129	66049	1	Phaeo
0.040196	0.066136	66764	1	TBB
0.025923	0.052249	67756	1	%Chl

2024). Further, the mucopolysaccharides excreted by Phaeocystis are a potential hotspot for bacteria (Alderkamp et al. 2007), which might be a contributing factor to the increased TBN and TBB from 2016 to 2019. The overall change in phytoplankton composition over the investigated time series likely also affected the composition of benthic bacterial communities. An ex situ experiment at HAUSGARTEN showed that benthic bacteria actively responded to an input of organic matter by initiating decomposition and the production of biomass, with a significant increase in the relative abundances of certain bacterial taxa under phytodetritus treatment (Hoffmann et al. 2017). The increase in TBN and TBB from 2016 to 2019 in combination with the high phaeopigment concentration could therefore be a result of this process. Thus, the shift in phytoplankton composition and subsequent changes in bacterial numbers, biomass and potentially composition could directly affect nematode food availability and quality.

Temporal changes in food availability — specifically phytodetritus and bacteria — explained 15% of the taxonomic variation in HAUSGARTEN nematode communities, with phaeopigment concentration being the key predictor at HG-I in 2009, 2014, and 2019, and increased TBB best explaining variation at HG-IV and

HG-VII in 2019. Some uncertainty remains in the model, as bacterial data were only available for the uppermost centimetre of the sediments, the model only considers results for surface sediments, and the bacteria data for 2000 are only an average as they were not sampled in that year. Nevertheless, our model shows that the nematode communities at the different stations are influenced by different food parameters and that the importance of each parameter differs between stations.

We saw the biggest change in food quantity (and possibly quality) at HG-I, but nematode community structure changed at all stations, especially illustrated with the highest exchange ratios at HG-VII. It is likely that the effect of proportional lower food input with depth is enhanced by the steep seafloor inclination at HG-VII, resulting in less predictable and more unstable habitat conditions for the nematode communities. The high dispersion at HG-VII revealed by the PERMDISP further underscores a high hetero-

geneity of environmental conditions at abyssal depths of HAUSGARTEN in space and time. These findings suggest that, while food availability is a key driver at all stations, the specific type, dynamics, and delivery of food, coupled with topographic and hydrodynamic factors, likely explain the distinct responses observed across the depth gradient.

4.2. Changes in nematode abundance and community structure

The bathymetric decline in nematode abundance and α -diversity among the stations is related to reduced food availability with increasing water depth, which has already been reported in previous studies at the HAUSGARTEN observatory (Hoste et al. 2007, Grzelak et al. 2017, Soltwedel et al. 2020, Schnier et al. 2023) and is comparable to other deep-sea regions (Rex et al. 2006).

On the temporal scale, a conspicuous result of our study was the detection of significantly lower mean nematode abundances at all stations in 2014 and 2019, compared to the previous years (2000, 2004, 2009). Soltwedel et al. (2020) reported this general trend for major meiofaunal taxa (to which nematodes are the

main contributors) with interannual variations along the HAUSGARTEN bathymetric transect off Svalbard until the end of their study period in 2014. The present study shows that this decline in nematode abundances, most pronounced at HG-I and HG-IV, has continued and even intensified until 2019 and was accompanied by a shift in nematode diversity.

Deep-sea nematode communities generally show a high β -diversity. For example, Danovaro et al. (2009) found very high turnover in samples from the Northeast Atlantic and Western Mediterranean (although the authors used a different β -diversity estimator). In the present study, the evaluation of the nematode β diversity on the temporal scale revealed high turnover rates at HG-I with relatively constant α -diversity values between the respective 5 yr time periods of 2000, 2004, 2009, and 2014. This indicates that there has been a substitution of genera without an overall loss of diversity. The immigration of several new, initially rare genera could have caused the high GER_r values compared to the lower GER_a values (Hillebrand et al. 2018). In 2019, however, a high turnover with up to 59% exchange in genus identities (GER_r) and up to 30% change in genus dominance structure (GER_a) was identified. Further, at HG-I, a concurrent decrease in α -diversity to values lower than those found at HG-IV in any year indicates a profound change in the nematode communities.

At HG-IV, the difference between the GER_r (up to 55%) and GER_a (up to 12%) in 2019 was even higher than at HG-I, indicating that the number of rare genera at HG-IV also increased compared to 2014. At HG-VII, GER_r and GER_a were comparably high in 2004 and 2019, respectively, indicating that genus identity and dominance structure changed simultaneously (Hillebrand et al. 2018). However, due to missing data for 2009 and 2014, the exchange ratios may not be directly comparable to HG-I and HG-VII.

Increased mean GER values are expected when diversity change accumulates over time, as continuous change does not allow for the re-appearance of the initial genus composition (Hillebrand et al. 2018, Rishworth et al. 2020). The spatial comparison of mean GERs suggests that the nematode communities at HAUSGARTEN are generally characterised by a combination of immigration or replacement of rare genera, with less variation in the main dominance structure at the shallower stations HG-I and HG-IV. In contrast, HG-VII is characterised by a simultaneous shift in the identity of genera and their relative proportions in the total nematode community.

It should be noted that the risk of induced artificial diversity through misidentifications caused by different investigators, which is potentially inherent in all long biological time-series studies, was of course also a factor in the present study, since the nematode genera from 2000-2009 and 2010-2019 were determined by 3 different investigators. However, skill level of the determinants was comparable and images of nematode genera obtained from the 2000-2009 data set were used as a reference in addition to the literature (see Section 2.1.2) for the 2010-2019 data set determinations, thereby minimising the risk of taxonomy bias. In addition, it should be mentioned that there are samples available for each year of the long-term time series of HAUSGARTEN from the year 2000 to the year 2019. However, most of these samples have not been analysed at the nematode genus level due to the time-consuming sample preparation and identification process, as well as limited personnel capacities. Therefore, we have chosen here to analyse the data at 5 yr intervals to represent the time series. Filling these time gaps is certainly a goal for the future as our study shows that the deep-sea nematode communities at HAUSGARTEN have changed substantially over 20 yr, with the shallower stations becoming more similar to the deeper stations in terms of abundance and diversity. Whether this change indicates decline of habitat conditions or food quality or is due to natural variation remains uncertain. Investigations of nematode genus data at shorter time intervals, ideally (inter-) annually, combined with a spatial increase, i.e. more stations along the bathymetric transect, could address this issue. Furthermore, functional diversity should also be investigated in more detail over the entire time series as there is evidence that the diversity of nematode feeding types at HAUSGARTEN changes with sediment depth, water depth and over time (Schnier et al. 2023, J. Schnier & C. Hasemann unpubl. data), which might have implications on the overall ecological functioning of deep sea meiofauna.

4.3. Changes in nematode biomass

Size spectra were investigated as a measure of the functional structure of the nematode communities (Schwinghamer 1981, 1983). The distribution of biomass across size classes can provide insights into the dominant life history strategies within a community. For instance, a peak in biomass in larger size classes may indicate the dominance of larger, long-lived K-strategists, whereas a higher proportion of biomass in smaller size classes could suggest the prevalence of smaller, short-lived r-strategists in the community. Our findings indicated a general decrease in total

nematode biomass with increasing water depth, which is a consistent pattern for deep-sea meiofauna (Wei et al. 2010). Food scarcity and its patchy distribution could favour r-strategists in abyssal sediments, as a broad niche space, fast generation times and high dispersal rates are essential for exploiting new food sources (Bongers 1990).

When observed over time, it is conspicuous that the lower end of the size-class spectrum in 2019 did not extend below size class -8, whereas in other years the observed spectrum ranged to -11, which was especially evident at HG-VII. Individual biomass was higher in 2019 compared to 2014 at all stations and was accompanied by a higher ratio of adults to juveniles (Figs. S2 & S3), which would explain the higher biomass of larger nematodes in 2019.

It seems probable that differences in the age structure of the community may have caused the variation in the biomass of the investigated genera. Soltwedel et al. (1996) provided evidence that the life cycle of deep-sea nematodes (and therefore also their size spectra) might be subjected to variability induced by pulses of organic matter input, hence the difference in sampling seasonality between 2014 and 2019 may be reflected in the age structure. Additionally, Vanaverbeke et al. (2004) found that the increase in abundance of short, stout nematodes like *Desmoscolex* and *Tricoma* was most pronounced after an input of organic matter, which is consistent with our findings at HG-I in 2019.

5. CONCLUSIONS

Environmental conditions in Fram Strait have changed considerably in the first 2 decades of this millennium. Long-term analysis revealed that the change is not only restricted to processes in the upper water column but that it propagated and significantly affected the deep meiobenthic nematode communities in terms of their food supply, abundance, community structure and diversity. While the effect of water depth on the nematode communities was larger than the effect of time and most pronounced in shallower depths, the effect of time was still clearly discernible, progressive and significant across all depths. With the ongoing rapid change in the Arctic Ocean and increasing anthropogenic activities in the deep sea, this often-considered stable ecosystem is experiencing increasing pressure. The continuation and intensification of the HAUSGARTEN time-series investigations could provide a unique baseline for a better understanding of processes in a polar deep-sea ecosystem.

Data availability. Nematode count or abundance data, as well as biomass data are archived in 2 data sets at PANGAEA (Schnier et al. 2025a,b). A harmonized, curated version of the data sets is also available in the CRITTERBASE data warehouse (Teschke et al. 2022). The HAUSGARTEN time series data on biogenic parameters for the years 2000—2015 are accessible on Mendeley Data (Hasemann & Soltwedel 2024); for 2016—2019, see Part 1 of Supplement 1.

Acknowledgements. We greatly thank the RV 'Polarstern' captains, crews, cruise leaders and all other involved persons of the expeditions ARK-XVI, ARK-XX/1, ARK-XXIV/2, PS85, PS121 and all other HAUSGARTEN cruises, without whom our data set would not exist. We are much obliged to Anja Pappert and the deep-sea volunteers (FÖJ participants) for analysing the environmental parameters and for their assistance with sample preparation. Special thanks also to Jule Wirries, who patiently carried out size measurements for hundreds of nematodes that were examined in this study. We express our gratitude to Dorothee Hodapp, who kindly provided a detailed R markdown for the β-diversity analyses, which was a tremendous help. Many thanks also to Lilian Böhringer for the help with QGIS. Furthermore, we thank the 3 anonymous reviewers, whose critical input significantly improved this paper. This research did not receive any specific grant from funding agencies in the public, commercial or not-for-profit sectors. We explicitly acknowledge the support by the Open Access Publication Funds of the Alfred-Wegener-Institute Helmholtz-Centre for Polar and Marine Research. The present work is part of J.S.'s PhD thesis.

LITERATURE CITED

Alderkamp AC, Buma AGJ, van Rijssel M (2007) The carbohydrates of *Phaeocystis* and their degradation in the microbial food web. In: van Leeuwe MA, Stefels J, Belviso S, Lancelot C, Verity PG, Gieskes WWC (eds) *Phaeocystis*, major link in the biogeochemical cycling of climate-relevant elements. Springer, Dordrecht, p 99−118

Anderson M, Gorley RN, Clarke KR (2008) Permanova+ for PRIMER: guide to software and statistical methods. Primer-E, Plymouth

Andrássy I (1956) Die Rauminhalts- und Gewichtsbestimmung der Fadenwürmer (Nematoden). Acta Zool Hung 2: 1-5

Aphalo PJ (2022) ggpmisc: miscellaneous extensions to 'ggplot2'. R package version 0.5.2. https://CRAN.R-project.org/package=ggpmisc

Armenteros M, Quintanar-Retama O, Gracia A (2022)
Depth-related patterns and regional diversity of freeliving nematodes in the deep-sea Southwestern Gulf of
Mexico. Front Mar Sci 9:1023996

Baguley JG, Montagna PA, Hyde LJ, Rowe GT (2008) Metazoan meiofauna biomass, grazing, and weight-dependent respiration in the Northern Gulf of Mexico deep sea. Deep Sea Res II 55:2607–2616

Bauerfeind E, Nöthig EM, Beszczynska A, Fahl K and others (2009) Particle sedimentation patterns in the eastern Fram Strait during 2000–2005: results from the Arctic long-term observatory HAUSGARTEN. Deep Sea Res I 56:1471–1487

Beszczynska-Möller A, Fahrbach E, Schauer U, Hansen E (2012) Variability in Atlantic water temperature and

- transport at the entrance to the Arctic Ocean, 1997—2010. ICES J Mar Sci 69:852-863
- Bluhm BA, Ambrose WG Jr, Bergmann M, Clough LM and others (2011) Diversity of the Arctic deep-sea benthos.

 Mar Biodivers 41:87–107
- *Bongers T (1990) The maturity index: an ecological measure of environmental disturbance based on nematode species composition. Oecologia 83:14–19
- Børsheim KY, Bratbak G, Heldal M (1990) Enumeration and biomass estimation of planktonic bacteria and viruses by transmission electron microscopy. Appl Environ Microbiol 56:352—356
- Bratbak G (1985) Bacterial biovolume and biomass estimations. Appl Environ Microbiol 49:1488—1493
- Budéus G, Lemke P (2007) The expeditions ARKTIS-XX/1 and ARKTIS-XX/2 of the research vessel Polarstern in 2004. Alfred-Wegener-Institut für Polar- und Meeresforschung, Bremerhaven
 - Clarke KR, Gorley RN (2006) PRIMER v6: user manual/tutorial (Plymouth routines in multivariate ecological research). PRIMER-e, Plymouth
- Coull BC (1999) Role of meiofauna in estuarine soft-bottom habitats. Aust J Ecol 24:327—343
- To Danovaro R, Bianchelli S, Gambi C, Mea M, Zeppilli D (2009) α-, β-, γ-, δ- and ε-diversity of deep-sea nematodes in canyons and open slopes of Northeast Atlantic and Mediterranean margins. Mar Ecol Prog Ser 396:197—209
- Danovaro R, Carugati L, Corinaldesi C, Gambi C, Guilini K, Pusceddu A, Vanreusel A (2013) Multiple spatial scale analyses provide new clues on patterns and drivers of deep-sea nematode diversity. Deep Sea Res II 92:97—106
- Dunn OJ (1961) Multiple comparisons among means. J Am Stat Assoc 56:52–64
- Fadeev E, Rogge A, Ramondenc S, Nöthig EM and others (2021) Sea ice presence is linked to higher carbon export and vertical microbial connectivity in the Eurasian Arctic Ocean. Commun Biol 4:1255
- GEBCO Bathymetric Compilation Group (2023) The GEBCO_2023 grid—a continuous terrain model of the global oceans and land. NERC EDS British Oceanographic Data Centre NOC
- Gerlach SA (1978) Food-chain relationships in subtidal silty sand marine sediments and the role of meiofauna in stimulating bacterial productivity. Oecologia 33:55–69
- Graf G (1989) Benthic-pelagic coupling in a deep-sea benthic community. Nature 341:437–439
 - Grzelak KA (2015) Structural and functional diversity of Nematoda at the Arctic deep-sea long-term observatory HAUSGARTEN (Fram Strait). PhD dissertation, Polish Academy of Sciences, Sopot
- Grzelak K, Kotwicki L, Hasemann C, Soltwedel T (2017)
 Bathymetric patterns in standing stock and diversity of
 deep-sea nematodes at the long-term ecological research
 observatory HAUSGARTEN (Fram Strait). J Mar Syst
 172:160–177
- Guden RM, Haegeman A, Ruttink T, Moens T, Derycke S (2024) Nematodes alter the taxonomic and functional profiles of benthic bacterial communities: a metatranscriptomic approach. Mol Ecol 33:e17331
- Hasemann C, Soltwedel T (2024) LTER HAUSGARTEN data on biogenic sediment compounds from 1999 to 2015. https://doi.org/10.17632/h8r8j3v59j.1
 - Heip C, Vincx M, Vranken G (1985) The ecology of marine nematodes. Oceanogr Mar Biol Annu Rev 23:399–489
- Hesterberg T (2022) resample: resampling functions. R pack-

- age version 0.6. https://CRAN.R-project.org/package=resample
- **Hillebrand H, Blasius B, Borer ET, Chase JM and others (2018) Biodiversity change is uncoupled from species richness trends: consequences for conservation and monitoring. J Appl Ecol 55:169—184
- M, Bienhold C (2017) Response of bacterial communities to different detritus compositions in Arctic deep-sea sediments. Front Microbiol 8:266
- *Holm-Hansen O, Lorenzen CJ, Holmes RW, Strickland JDH (1965) Fluorometric determination of chlorophyll. ICES J Mar Sci 30:3—15
- Hoste E, Vanhove S, Schewe I, Soltwedel T, Vanreusel A (2007) Spatial and temporal variations in deep-sea meiofauna assemblages in the Marginal Ice Zone of the Arctic Ocean. Deep Sea Res I 54:109—129
- Hurlbert SH (1971) The nonconcept of species diversity: a critique and alternative parameters. Ecology 52:577–586
- Tingels J, Van den Driessche P, De Mesel I, Vanhove S, Moens T, Vanreusel A (2010) Preferred use of bacteria over phytoplankton by deep-sea nematodes in polar regions.

 Mar Ecol Prog Ser 406:121–133
- Ingels J, Billett DSM, Van Gaever S, Vanreusel A (2011) An insight into the feeding ecology of deep-sea canyon nematodes results from field observations and the first insitu ¹³C feeding experiment in the Nazaré Canyon. J Exp Mar Biol Ecol 396:185—193
- Jaccard P (1912) The distribution of the flora in the alpine zone. New Phytol 11:37–50
- Jensen P (1988) Nematode assemblages in the deep-sea benthos of the Norwegian Sea. Deep-Sea Res A 35:1173—1184
- Kassambara A (2023a) ggpubr: 'ggplot2' based publication ready plots. R package version 0.6.1. https://CRAN.R-project.org/package=ggpubr
- Kassambara A (2023b) rstatix: pipe-friendly framework for basic statistical tests. R package version 0.7.2. https://CRAN.R-project.org/package=rstatix
- *Klages M (2010) The expedition of the research vessel Polarstern to the Arctic in 2009 (ARK-XXIV/2). Alfred-Wegener-Institut für Polar- und Meeresforschung, Bremerhaven
- Klenke M, Schenke HW (2002) A new bathymetric model for the central Fram Strait. Mar Geophys Res 23:367–378
- Knust R (2017) Polar research and supply vessel POLAR-STERN operated by the Alfred-Wegener-Institute. J Large-Scale Res Facil 3:A119
- Krause G, Schauer U (2001) The expeditions ARKTIS XVI/1 and ARKTIS XVI/2 of the research vessel Polarstern in 2000. Alfred-Wegener-Institut für Polar- und Meeresforschung, Bremerhaven
- Kruskal WH, Wallis WA (1952) Use of ranks in one-criterion variance analysis. J Am Stat Assoc 47:583—621
- Lalande C, Bauerfeind E, Nöthig EM, Beszczynska-Möller A (2013) Impact of a warm anomaly on export fluxes of biogenic matter in the eastern Fram Strait. Prog Oceanogr 109:70–77
- Metfies K (2020) The expedition PS121 of the research vessel POLARSTERN to the Fram Strait in 2019. Alfred-Wegener-Institut, Helmholtz-Zentrum für Polar- und Meeresforschung, Bremerhaven
 - Montagna PA (1995) Rates of metazoan meiofauna microbivory: a review. Vie Milieu 45:1–9
- Nemys Eds. (2023) Nemys: World Database of Nematodes. https://nemys.uqent.be

- Nöthig EM, Bracher A, Engel A, Metfies K and others (2015) Summertime plankton ecology in Fram Strait — a compilation of long- and short-term observations. Polar Res 34: 23349
- Nöthig EM, Ramondenc S, Haas A, Hehemann L and others (2020) Summertime chlorophyll *a* and particulate organic carbon standing stocks in surface waters of the Fram Strait and the Arctic Ocean (1991–2015). Front Mar Sci 7:350
 - Pfannkuche O, Thiel H (1988) Sample processing. In: Higgins RP, Thiel H (eds) Introduction to the study of meiofauna. Smithsonian Institution Press, Washington, DC, p 134–145
- Pielou EC (1966) The measurement of diversity in different types of biological collections. J Theor Biol 13:131—144
 - Platt HM, Warwick RM (1983) Freeliving marine nematodes. Part I: British Enoplids. Pictorial key to world genera and notes for the identification of British species. Cambridge University Press, Cambridge
 - Platt HM, Warwick RM (1988) Freeliving marine nematodes. Part II: British Chromadorids. Pictorial key to world genera and notes for identification of British species. Cambridge University Press, Leiden
- Posit Team (2023) RStudio: integrated development environment for R. www.posit.co/
- ズQGIS Development Team (2009) QGIS Geographic Information System. http://qgis.osgeo.org
- Qiu Y (2023) showtext: using fonts more easily in R graphs.
 R package version 0.9.7. https://CRAN.R-project.org/package=showtext
 - Core Team (2023) R: a language and environment for statistical computing. R Foundation for Statistical Computing, Vienna
- Ramirez-Llodra E, Meyer HK, Bluhm BA, Brix S and others (2024) The emerging picture of a diverse deep Arctic Ocean seafloor: from habitats to ecosystems. Elementa Sci Anthropocene 12:00140
- Ramondenc S, Iversen MH, Soltwedel T (2024) Long-term measurements reveal a 100-day lag between peaks in phytoplankton chlorophyll and benthic bacterial abundance in the Fram Strait. ICES J Mar Sci 81:1647—1654
- Rex MA, Etter RJ, Morris JS, Crouse J and others (2006) Global bathymetric patterns of standing stock and body size in the deep-sea benthos. Mar Ecol Prog Ser 317: 1–8
- Riebesell U, Reigstad M, Wassmann P, Noji T, Passow U (1995) On the trophic fate of *Phaeocystis pouchetii* (Hariot): VI. Significance of *Phaeocystis*-derived mucus for vertical flux. Neth J Sea Res 33:193–203
- Rishworth GM, Adams JB, Bird MS, Carrasco NK and others (2020) Cross-continental analysis of coastal biodiversity change. Philos Trans R Soc B 375:20190452
- Rudis B (2020) hrbrthemes: additional themes, theme components and utilities for 'ggplot2'. R package version 0.8.7. https://CRAN.R-project.org/package=hrbrthemes
- Sanders HL (1968) Marine benthic diversity: a comparative study. Am Nat 102:243–282
- Schewe I (2015) The expedition PS85 of the research vessel POLARSTERN to the Fram Strait in 2014. Alfred-Wegener-Institut, Helmholtz-Zentrum für Polar- und Meeresforschung, Bremerhaven
- Schmidt-Rhaesa A (ed) (2014) Handbook of zoology. Gastrotricha, Cycloneuralia and Gnathifera. De Gruyter, Berlin
- Schnier J, Hasemann C, Mokievsky V, Martínez Arbizu P, Soltwedel T (2023) Nematode communities along a bathymetric transect in the deep eastern Fram Strait

- (Arctic Ocean): interrelations between diversity, function and environment. Front Mar Sci 10:1271447
- Schnier J, Grzelak K, Hasemann C, Soltwedel T (2025a) Data on nematode genus abundance and counts at LTER HAUSGARTEN from 2000 to 2009, 2010, 2014 and 2019. https://doi.pangaea.de/10.1594/PANGAEA.973147
- Schnier J, Hasemann C, Soltwedel T (2025b) Data on nematode genus, body size, biomass, feeding types, tail shapes and cp-values at LTER HAUSGARTEN from 2010, 2014 and 2019. https://doi.pangaea.de/10.1594/PANGAEA. 973148
- Schratzberger M, Ingels J (2018) Meiofauna matters: the roles of meiofauna in benthic ecosystems. J Exp Mar Biol Ecol 502:12–25
- Schwinghamer P (1981) Characteristic size distributions of integral benthic communities. Can J Fish Aquat Sci 38: 1255–1263
- Schwinghamer P (1983) Generating ecological hypotheses from biomass spectra using causal analysis: a benthic example. Mar Ecol Prog Ser 13:151–166
- Shannon CE (1948) A mathematical theory of communication. Bell Syst Tech J 27:379—423
- Shimanaga M, Shirayama Y (2000) Response of benthic organisms to seasonal change of organic matter deposition in the bathyal Sagami Bay, central Japan. Oceanol Acta 23:91–107
- Smith CR, De Leo FC, Bernardino AF, Sweetman AK, Martínez Arbizu P (2008) Abyssal food limitation, ecosystem structure and climate change. Trends Ecol Evol 23: 518–528
- Soetaert K, Heip C (1995) Nematode assemblages of deepsea and shelf break sites in the North Atlantic and Mediterranean Sea. Mar Ecol Prog Ser 125:171–183
- Soltwedel T, Pfannkuche O, Thiel H (1996) The size structure of deep-sea meiobenthos in the North-Eastern Atlantic: nematode size spectra in relation to environmental variables. J Mar Biol Assoc UK 76:327–344
- Soltwedel T, Bauerfeind E, Bergmann M, Budaeva N and others (2005) HAUSGARTEN: multidisciplinary investigations at a deep-sea, long-term observatory in the Arctic Ocean. Oceanography 18:46–61
- Soltwedel T, Bauerfeind E, Bergmann M, Bracher A and others (2016) Natural variability or anthropogenically-induced variation? Insights from 15 years of multidisciplinary observations at the Arctic marine LTER site HAUSGARTEN. Ecol Indic 65:89–102
- Soltwedel T, Grzelak K, Hasemann C (2020) Spatial and temporal variation in deep-sea meiofauna at the LTER Observatory HAUSGARTEN in the Fram Strait (Arctic Ocean). Diversity 12:279
- Strugger S (1948) Fluorescence microscope examination of bacteria in soil. Can J Res 26:188–193
- Swoboda S, Krumpen T, Nöthig EM, Metfies K and others (2024) Release of ballast material during sea-ice melt enhances carbon export in the Arctic Ocean. PNAS Nexus 3:pqae081
- Teschke K, Kraan C, Kloss P, Andresen H and others (2022) CRITTERBASE, a science-driven data warehouse for marine biota. Sci Data 9:483
- Vanaverbeke J, Soetaert K, Vincx M (2004) Changes in morphometric characteristics of nematode communities during a spring phytoplankton bloom deposition. Mar Ecol Prog Ser 273:139–146
- Vanhove S, Wittoeck J, Desmet G, Van den Berghe B and others (1995) Deep-sea meiofauna communities in Ant-

- arctica: structural analysis and relation with the environment. Mar Ecol Proq Ser 127:65-76
- Vanhove S, Vermeeren H, Vanreusel A (2004) Meiofauna towards the South Sandwich Trench (750–6300 m), focus on nematodes. Deep Sea Res II 51:1665–1687
- Vihtakari M (2023) ggOceanMaps: plot data on oceanographic maps using 'ggplot2'. R package version 2.2.0. https://mikkovihtakari.github.io/ggOceanMaps/
 - Warwick RM, Platt HM, Somerfield PJ (1998) Freeliving marine nematodes. Part III: Monhysterids. Pictorial key to world genera and notes for the identification of British species. The Linnean Society of London and the Estuarine and Coastal Sciences Association, Shrewsbury
- Wei CL, Rowe GT, Escobar-Briones E, Boetius A and others (2010) Global patterns and predictions of seafloor biomass using random forests. PLOS ONE 5:e15323
- Wickham H, Averick M, Bryan J, Chang W and others (2019) Welcome to the tidyverse. J Open Source Softw 4:1686
- Wieser W (1960) Benthic studies in Buzzards Bay II. The meiofauna, Limnol Oceanogr 5:121–137

Editorial responsibility: Deborah K. Steinberg, Gloucester Point, Virginia, USA Reviewed by: T. Pereira, E. Baldrighi and 1 anonymous referee Submitted: December 20, 2024; Accepted: July 11, 2025 Proofs received from author(s): September 30, 2025

- Wilke CO (2020) cowplot: streamlined plot theme and plot annotations for 'ggplot2'. R package version 1.2.0. https://CRAN.R-project.org/package=cowplot
- Wolf KKE, Hoppe CJM, Rehder L, Schaum E, John U, Rost B (2024) Heatwave responses of Arctic phytoplankton communities are driven by combined impacts of warming and cooling. Sci Adv 10:eadl5904
- Wolff T (1977) Diversity and faunal composition of the deepsea benthos. Nature 267:780—785
- Wollenburg JE, Katlein C, Nehrke G, Nöthig EM and others (2018) Ballasting by cryogenic gypsum enhances carbon export in a *Phaeocystis* under-ice bloom. Sci Rep 8:7703
- Yentsch CS, Menzel DW (1963) A method for the determination of phytoplankton chlorophyll and phaeophytin by fluorescence. Deep-Sea Res Oceanogr Abstr 10: 221–231
- Zeppilli D, Sarrazin J, Leduc D, Arbizu PM and others (2015) Is the meiofauna a good indicator for climate change and anthropogenic impacts? Mar Biodivers 45:505—535

This article is Open Access under the Creative Commons by Attribution (CC-BY) 4.0 License, https://creativecommons.org/licenses/by/4.0/deed.en. Use, distribution and reproduction are unrestricted provided the authors and original publication are credited, and indicate if changes were made